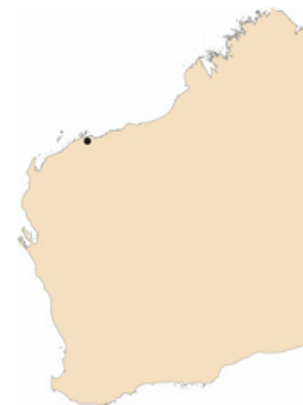


201973: gold grain, Nickol River prospect (Ruth Well Formation, Karratha Terrane)

| | |
|----------------------------|---|
| Sample type | Gold grain |
| Total weight | 0.6 g |
| Sample location | Nickol River prospect, about 13 km east of Karratha |
| Coordinates | MGA zone 50, 496108E 7705957N |
| Datum | GDA94 |
| 1:250 000 map sheet | DAMPIER (SF 50-2) |
| 1:100 000 map sheet | DAMPIER (2256) |
| Tenement | E 47/2716 |
| Collector | Artemis Resources |



Location and sampling

The sample was provided by Artemis Resources in January 2019. It was collected from surface scrapings above sheared ultramafic rocks and a quartz vein, at the Nickol River prospect in the northwest Pilbara region (Artemis Resources, 2019, written comm., 11 January).

Geological context

The Nickol River prospect is located about 1.1 km south-southeast of the northern segment of the Regal Thrust, in the Roebourne greenstone belt of the Karratha Terrane, northwest Pilbara Craton. The Regal Thrust is a regionally significant fault known to be spatially associated with Cu–Au mineralization (Hickman, 2016; GSWA, 2020). The local bedrock includes metamorphosed serpentized peridotite with sporadically preserved olivine–spinel textures, and minor serpentine–chlorite schist of the 3280–3261 Ma Ruth Well Formation, Roebourne Group (Hickman, 2022; GSWA, 2020).

The Nickol River prospect lies immediately west of the historical Nickol River gold mining area, which has produced alluvial gold from 1889 to the present day, that was potentially derived from a nearby, outcropping bedrock-hosted primary hydrothermal gold mineralization (Cyclone Metals Ltd, 2022).

The nearest regolith landform is an alluvial–fluvial unit comprising unconsolidated clay, silt, sand, and basaltic or doleritic gravel on a floodplain. Expanding clays locally form a gilgai surface (GSWA, 2020).

Methodology

The gold sample was photographed and weighed, and its overall morphology and external features, such as colour, roundness, surface relief, coatings, mineral inclusions and mineralogical assemblages were recorded using

visual morphometry. The raw surface of the sample was analysed using scanning electron microscopy with energy dispersive X-ray system (SEM-EDS). The sample was then mounted in epoxy resin, cut and polished and the gold grain microstructure and inclusions were examined using optical and SEM-EDS analyses. Gold microchemistry was determined by laser ablation inductively coupled plasma mass spectrometry (LA-ICP-MS), calibrated against certified gold reference materials (CRM; Murray, 2009). The sample was ablated in triplicate along 0.5 mm-long traverses and average values calculated for elements present in the CRM. The gold surface was repolished after laser ablation, etched with aqua regia, and its internal structure examined using reflected light microscopy and SEM-EDS. Details of this method are described in Hancock and Beardsmore (2020).

Morphology

The gold grain is well rounded but irregular, with dimensions $8 \times 6 \times 1.5$ mm. It is covered by ferruginous clays (Fig. 1).



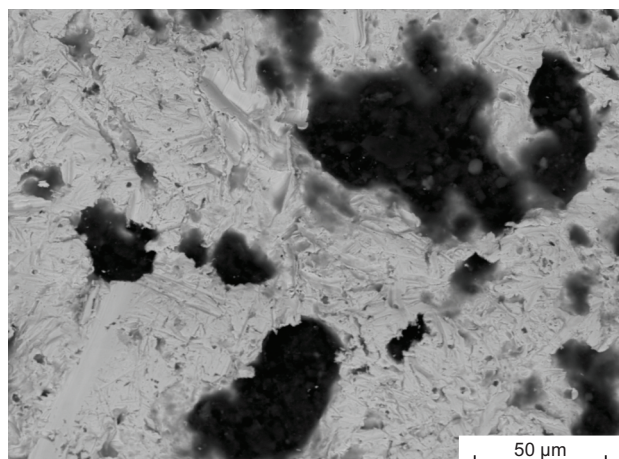
EAH214

25.03.22

Figure 1. Sample 201973: gold grain, Nickol River prospect

SEM-EDS analysis of raw surfaces

The surface of the gold grain is extensively scratched and pitted (Fig. 2), and contains no detectable Ag. Pits are partially filled with Al-Fe-Mg clays with minor Ca and K, and small angular quartz grains. Gold nanoparticles are sporadically disseminated in the clays.



EAH215 30.03.22

Figure 2. Backscattered electron image of sample 201973: gold grain, Nickol River prospect

Optical microscopy of polished surfaces

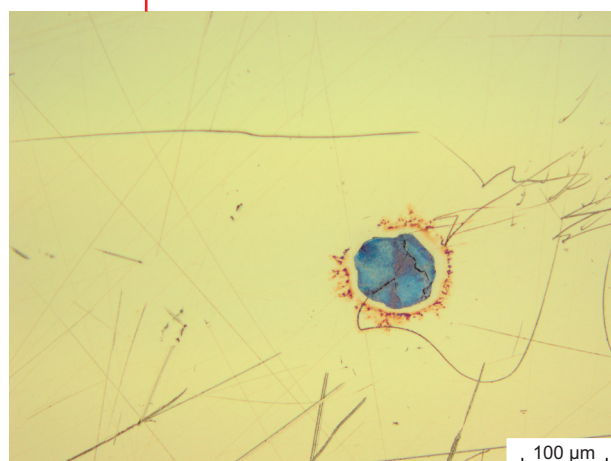
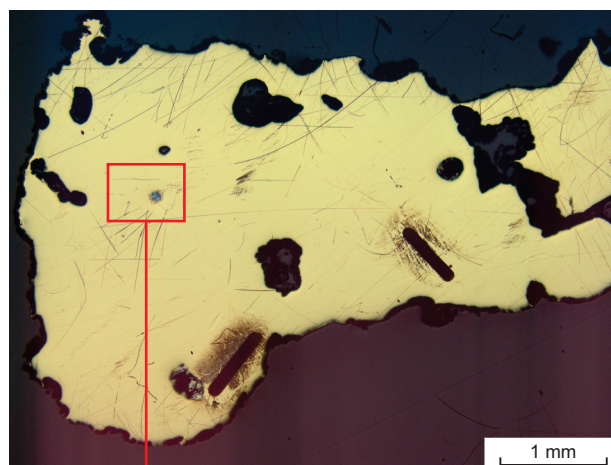
In section, the locally cavernous nature of the grain margin is evident, indicating some dissolution of gold. The voids are filled by regolith material. The interior of the grain is largely massive gold with large voids and a small rounded inclusion of chalcopyrite showing colourful heterogenic phases (Fig. 3).

SEM-EDS analysis of polished surfaces

The massive gold contains 6–7% Ag, and several rounded inclusions of chalcopyrite 50–300 µm in diameter (Fig. 4a–c). The chalcopyrite contains up to 0.5% Ni, but generally only traces of Ag and no gold (Spectrum 120, Fig. 4a; Spectrum 123, Fig. 4c), though some inclusions contain irregular gold nanoparticles with up to 13% Ag (Spectrum 132 and 133, Fig. 4b), or have domains that are paler (under SEM) or contain abundant diffuse, pale spots, where Ag concentration ranges up to 27% (Spectrum 118 and 119, Fig. 4a). Oscillatory growth banding is sporadically present showing small variations in Fe, Ag and Zn (Spectrum 134 and 135, Fig. 4b). One chalcopyrite inclusion contains a 50 µm, blocky ankerite (Ca, Mg, Fe, Mn; Spectrum 126, Fig. 4b).

LA-ICP-MS analysis

Analyses consistently detected Ag, Cu and Hg within the gold grain, in concentrations higher than the instrument detection limit, probably occurring as limited solid solutions in the gold. Other trace elements were detected only sporadically in low (sub-ppm) concentrations, possibly occurring in micro- and nano-inclusions.



EAH216 25.03.22

Figure 3. Reflected-light photomicrographs of polished surface of sample 201973: gold grain, Nickol River prospect. Dark, elongate lines are laser ablation tracks produced during LA-ICP-MS analyses

The gold contains moderate Ag (6–7%) and Cu (506–630 ppm), and low Hg (22–27 ppm) (Table 1). Mg is present at sub-ppm concentrations, and very low (ppb) traces of Ti, Ni, Zn, As, Se, Pd, Sn, Sb, Pb and Bi were detected (Table 2).

Table 1. LA-ICP-MS data for selected elements in sample 201973: gold grain, Nickol River prospect

| Ag (%) | Cu (ppm) | Hg (ppm) | Minor elements |
|-----------------|---------------|------------|----------------|
| 6.3, 6.4, 7.087 | 506, 535, 630 | 22, 22, 27 | Mg |

Acid etching

The bulk of the gold grain is coarsely polycrystalline with strongly deformed (curved), simple twin planes (Fig. 5a). There is a variably developed marginal rim locally up to 300 µm thick that is recrystallized to finer-grained, randomly-oriented gold subgrains (Fig. 5b). There is locally a very thin (5–10 µm) mantle of Ag-free gold subgrains rimming the grain margin and (leached) inclusions, indicating modification of the gold by solution processes (Fig. 5a).

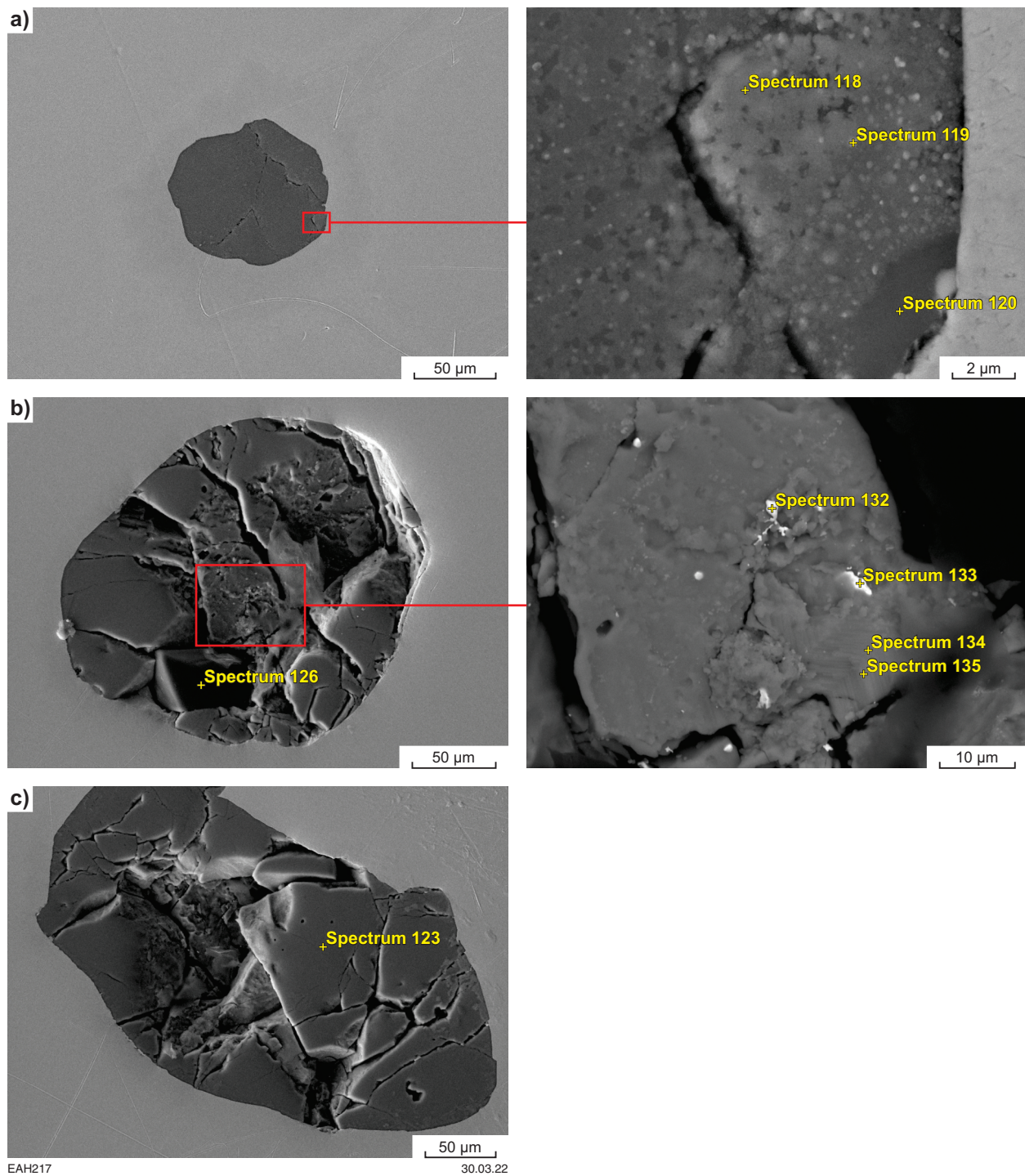


Figure 4. Backscattered electron (BSE) and secondary electron (SE) images of mineral inclusions in sample 201973: gold grain, Nickol River prospect: a) BSE; b) SE; c) SE

Table 2. LA-ICP-MS compositional data for sample 201973: gold grain, Nickol River prospect

| <i>Laser ablation track</i> | <i>Unit</i> | ⁷ Li | ⁹ Be | ¹¹ B | ²³ Na | ²⁵ Mg | ²⁷ Al | ²⁹ Si | ⁴⁴ Ca | ⁴⁵ Sc | ⁴⁹ Ti | ⁵¹ V | ⁵³ Cr | ⁵⁵ Mn | ⁵⁷ Fe | ⁵⁹ Co | ⁶⁰ Ni | ⁶⁵ Cu |
|-----------------------------|-------------|-----------------|-----------------|-----------------|------------------|------------------|------------------|------------------|------------------|------------------|------------------|-----------------|------------------|------------------|------------------|------------------|------------------|------------------|
| 1 | cps | | 1 | | | 34 | 24 | | | | 4 | 4 | 10 | | 3 | 8 | 8 | 62596 |
| 2 | cps | | | | | 36 | 98 | | | | | 4 | 117 | | | 6 | 5 | 66273 |
| 3 | cps | | 2 | | | 80 | 104 | | | | 4 | 2 | 4 | | | 4 | 4 | 77950 |
| 1 | ppm | | | | | 0.41 | | | | | 0.08 | | | | | | 0.08 | 506 |
| 2 | ppm | | | | | 0.43 | | | | | | | | | | | 0.05 | 535 |
| 3 | ppm | | | | | 0.96 | | | | | 0.08 | | | | | | 0.04 | 630 |

| <i>Laser ablation track</i> | <i>Unit</i> | ⁶⁶ Zn | ⁶⁹ Ga | ⁷² Ge | ⁷⁵ As | ⁸² Se | ⁸⁵ Rb | ⁸⁸ Sr | ⁸⁹ Y | ⁹⁰ Zr | ⁹³ Nb | ⁹⁸ Mo | ¹⁰¹ Ru | ¹⁰³ Rh | ¹⁰⁸ Pd | ¹⁰⁹ Ag | ¹¹¹ Cd | ¹¹⁵ In |
|-----------------------------|-------------|------------------|------------------|------------------|------------------|------------------|------------------|------------------|-----------------|------------------|------------------|------------------|-------------------|-------------------|-------------------|-------------------|-------------------|-------------------|
| 1 | cps | 11 | | | 6 | 1 | | 7 | | | | | | 2 | 5 | 13087076 | 24 | |
| 2 | cps | 11 | | | | 5 | | 6 | | | | 1 | | 3 | 5 | 13111209 | 19 | 2 |
| 3 | cps | 11 | | 3 | 4 | | 1 | 15 | | | | | | 3 | 6 | 14484996 | 26 | |
| 1 | ppm | 0.12 | | | 0.07 | 0.12 | | | | | | | | 0.004 | 0.04 | 63499 | | |
| 2 | ppm | 0.12 | | | | 0.40 | | | | | | | | 0.006 | 0.03 | 63616 | | 0.003 |
| 3 | ppm | 0.13 | | | 0.05 | | | | | | | | | 0.006 | 0.05 | 70281 | | |

| <i>Laser ablation track</i> | <i>Unit</i> | ¹²⁰ Sn | ¹²¹ Sb | ¹²⁶ Te | ¹³³ Cs | ¹³⁸ Ba | ¹³⁹ La | ¹⁴⁰ Ce | ¹⁴¹ Pr | ¹⁴⁵ Nd | ¹⁵¹ Eu | ¹⁵⁷ Gd | ¹⁵⁹ Tb | ¹⁶² Dy | ¹⁶⁵ Ho | ¹⁶⁷ Er | ¹⁶⁹ Tm | ¹⁷² Yb | |
|-----------------------------|-------------|-------------------|-------------------|-------------------|-------------------|-------------------|-------------------|-------------------|-------------------|-------------------|-------------------|-------------------|-------------------|-------------------|-------------------|-------------------|-------------------|-------------------|---|
| 1 | cps | 8 | 18 | | 1 | 4 | | | | | | | 1 | | | | | | 2 |
| 2 | cps | 12 | 19 | | | 3 | 1 | 1 | | | | | | | | | | 1 | |
| 3 | cps | 19 | 28 | 2 | 6 | 6 | 1 | | 1 | 1 | | 2 | | | | 2 | 1 | | |
| 1 | ppm | 0.03 | 0.07 | | | | | | | | | | | | | | | | |
| 2 | ppm | 0.05 | 0.07 | | | | | | | | | | | | | | | | |
| 3 | ppm | 0.09 | 0.11 | 0.03 | | | | | | | | | | | | | | | |

| <i>Laser ablation track</i> | <i>Unit</i> | ¹⁷⁵ Lu | ¹⁷⁸ Hf | ¹⁸¹ Ta | ¹⁸² W | ¹⁸⁵ Re | ¹⁸⁹ Os | ¹⁹³ Ir | ¹⁹⁵ Pt | ²⁰² Hg | ²⁰⁵ Tl | ²⁰⁸ Pb | ²⁰⁹ Bi | ²³² Th | ²³⁸ U |
|-----------------------------|-------------|-------------------|-------------------|-------------------|------------------|-------------------|-------------------|-------------------|-------------------|-------------------|-------------------|-------------------|-------------------|-------------------|------------------|
| 1 | cps | | | | | | | | | 7964 | | 5 | 8 | | |
| 2 | cps | | | | | | | | | 6251 | 2 | 6 | 8 | | |
| 3 | cps | 2 | | | | | | | 1 | 6466 | 1 | | 6 | | |
| 1 | ppm | | | | | | | | | 27 | | 0.01 | 0.017 | | |
| 2 | ppm | | | | | | | | | 22 | | 0.02 | 0.016 | | |
| 3 | ppm | | | | | | | | 0.014 | 22 | | | 0.013 | | |

Notes: cps, count per second; ppm, parts per million

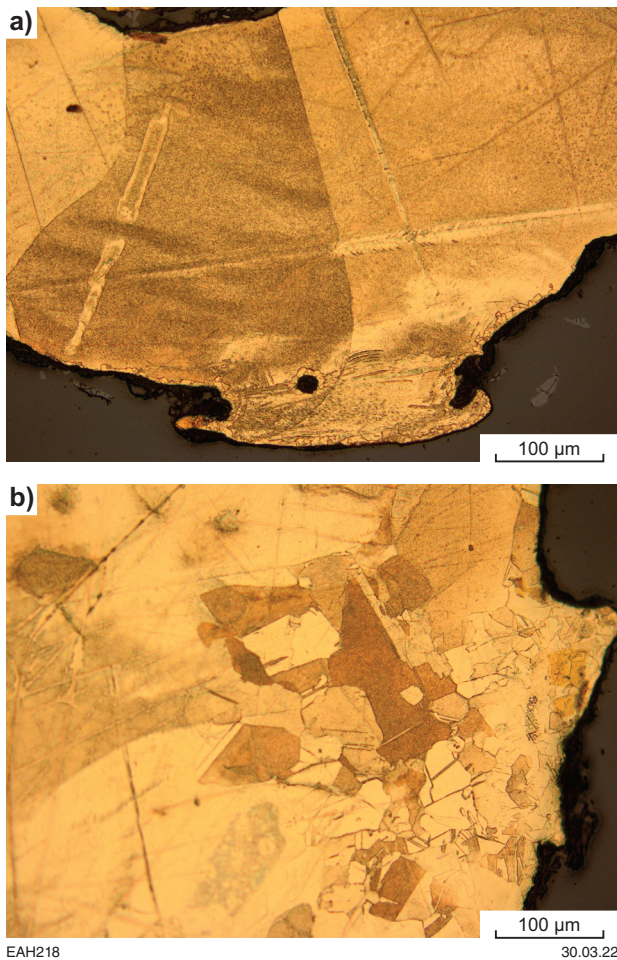


Figure 5. Reflected-light photomicrographs, after repolishing and acid etching, of parts of sample 201973: gold grain, Nickol River prospect

Interpretation

The gold containing 6–7% Ag and rounded chalcopyrite inclusions with high-Ag gold nanoparticles is probably of primary hydrothermal origin. The grain has been subsequently transported in the placer environment some distance from the primary source, during which time it has been deformed and partially recrystallized.

References

- Cyclone Metals Ltd 2022, Projects and Investments, Nickol River Gold Project: Cyclone Metals Ltd, viewed 14 April 2022, <<https://cyclonemetals.com/projects-investments/>>.
- Geological Survey of Western Australia 2020, Northwest Pilbara, 2020: Geological Survey of Western Australia, Geological Information Series, data package.
- Hancock, EA and Beardsmore, TJ 2020, Provenance fingerprinting of gold from the Kurnalpi Goldfield: Geological Survey of Western Australia, Report 212, 21p.
- Hickman, AH 2016, Northwest Pilbara Craton: A record of 450 million years in the growth of Archean continental crust: Geological Survey of Western Australia, Report 160, 104p.
- Hickman, AH 2022, Ruth Well Formation (A-ROR-xb-u): Geological Survey of Western Australia, WA Geology Online, Explanatory Notes extract, viewed 08 April 2022, <www.dmirs.wa.gov.au/ens>.
- Murray, S 2009, LBMA certified reference materials. Gold project final update: The London Bullion Market Association, Alchemist, no. 55, p. 11–12.

Recommended reference for this publication

- Hancock, EA, Blay, OA and Beardsmore, TJ 2023, 201973: gold grain, Nickol River prospect; GSWA Mineralogy Record 7: Geological Survey of Western Australia, 5p.